Oscillations in confined gases

O. L. de Lange and J. Pierrus
Department of Physics, University of Natal, Private Bag X01, Scottsville, Pietermaritzburg 3209, South Africa
(Received 23 December 1997)

We have used an electronic technique [J. Pierrus and O. L. de Lange, Phys. Rev. E **56**, 2841 (1997)] to monitor damped oscillations in Rüchardt's experiment for twelve gases (He, Ne, Ar, Kr, Xe, N_2, CO_2, N_2O, CHF_3, CCl_2F_2, SF_6, and C_2ClF_5) at room temperature and pressure. The nature of the oscillations depends on frequency (volume of gas) and amplitude. The bulk modulus K and relaxation time τ are measured over a range of volumes of gas (0.12–23 l: frequencies ~8–0.5 Hz) and amplitudes (6–0.01 cm). In gases for which C_p/C_v is not too low, there is evidence for an initial, transient adiabatic oscillation lasting one or two cycles. This is followed by a set of intermediate oscillations, which is observed for all gases, and can be studied in detail. For these oscillations, the agreement between experiment and theory is good. In particular, gases such as He and Ne exhibit high damping, whereas gases such as SF_6 and C_2ClF_5 have low damping, as predicted by theory. The intermediate oscillations are followed (as the amplitude decreases) by a second set of oscillations of constant, longer period. For the monatomic and diatomic gases the values of K and τ for these oscillations are consistent with isothermal oscillations, although the measurements of τ indicate the presence of residual thermal gradients at the higher frequencies (smaller volumes). For the polyatomic gases, measurements of τ yield a similar conclusion; however, values of K are lower than theoretical values for isothermal oscillations, and the disparity increases with the polyatomicity of the gas. In all gases, the amplitudes of oscillations in the isothermal tail increase as the frequency is decreased. [S1063-651X(98)06305-3]

PACS number(s): 51.30.+i, 51.40.+p, 44.10.+i, 05.60.+w

I. INTRODUCTION

Recently we described a sensitive electronic technique for studying oscillations in confined gases [1]. Our method is based on Rüchardt's well-known experiment for measuring the ratio of specific heats $\gamma = C_p/C_v$ of a gas [2]. This experiment uses a glass aspirator with a stopper through which passes a vertical, precision-made glass tube. A closely fitting, smooth steel ball is placed in the tube. If the ball is displaced from its equilibrium position and released, it performs a damped harmonic motion. By measuring the period of this motion (as the average of a number of cycles) and assuming that the oscillations of the gas are adiabatic, a value of γ can be obtained [2,3].

In our work we employed two modifications to this experiment. First, we used a linear voltage-displacement transducer to measure the displacement of the ball $x(t)$ very accurately. From the trace of $x(t)$ versus t we can accurately monitor the period T of each cycle. This period depends on the bulk modulus of the gas K according to

$$T = \left(\frac{4\pi^2 m V}{K A^2} \right)^{1/2}, \tag{1}$$

where m is the mass of the ball, V is the equilibrium volume of the gas, and A is the cross-sectional area of the tube [1]. Thus measurements of T for successive cycles enable one to study whether the bulk modulus of the gas is changing as the amplitude decreases due to damping. Also, using the same trace, one can obtain the relaxation time τ of the damped oscillations. The measurements of K and τ enable one to monitor the nature of the oscillations (whether they are adiabatic, isothermal, or intermediate between these extremes) [1].

The second modification [3] was to vary the volume of gas V by partially filling the aspirator with a suitable liquid (such as water or vacuum pump oil): this allows one to vary the frequency of the oscillations [see Eq. (1)]. Thus the gas we study is the ullage of the aspirator, and the equilibrium pressure of the gas is its partial pressure P in the aspirator. These two modifications enable us to monitor the oscillations of the gas as a function of the volume of gas (i.e., the frequency) and the amplitude of the oscillation. In our experiments, the volume of the gas was varied from about 0.12 l to about 23 l (the nominal volume of the aspirator is 20 l); the amplitude varied from about 6 cm down to about 0.01 cm.

One expects such measurements would show that the oscillations are not strictly adiabatic: clearly, due to the finite thermal conductivities of the gas and the glass walls, there must be heat flows out of and into the gas during the compression and expansion parts of the oscillations [4]. These will alter the temperature profile from that of an adiabatic oscillation, and we refer to such oscillations as intermediate between the adiabatic and isothermal extremes. In Ref. [1] we presented a detailed model of this behavior and showed that the bulk modulus and relaxation time are given by

$$K_m = \left(1 - \frac{3(\gamma - 1)a}{2\gamma R} \right) K_a \tag{2}$$

and [5]

$$\frac{1}{\tau_m} = \frac{1}{\tau_0} + D T^{-7/6}, \tag{3}$$

where

$$a=(\gamma\kappa T/\pi)^{1/2}, \tag{4}$$

$$D=12(\gamma-1)\left(\frac{\pi^3\kappa}{\gamma^{5/3}}\right)^{1/2}\left(\frac{2m}{3PA^2}\right)^{1/3}. \tag{5}$$

Here we have assumed, for convenience, a spherical aspirator of radius R and volume $V=\frac{4}{3}\pi R^3$. We have also assumed that the thermal conductivity of the glass walls is much larger than that of the gas. In the above, K_a is the bulk modulus for adiabatic oscillations of the gas: it is given by

$$K_a=\gamma PZ \tag{6}$$

with

$$Z=1+\frac{B(T)}{\overline{V}} \tag{7}$$

the usual compressibility factor ($\overline{V}$ is the molar volume) [6]. κ is the thermal diffusivity of the gas ($=\lambda/\rho C_p$ where λ is the thermal conductivity and ρ the density). In Eq. (3), the first term on the right-hand-side is associated with friction due to motion of the ball in the tube, and it is independent of the period T (see Sec. V and Appendix B); the second term, which does depend on T, is due to dissipation associated with heat flows in the oscillating gas.

In Ref. [1] we reported measurements of T and τ as functions of volume and amplitude for (synthetic) air at room temperature and pressure. The results showed unexpected features. One expects that, for a given volume of gas, the trace of $x(t)$ would yield values of T that are constant (apart from experimental scatter). However, the plots of $x(t)$ consisted of an initial set of cycles all with very nearly the same period, followed by a second set of cycles with a longer, nearly constant, period. The change in period between these two sets was accomplished quite rapidly, in just two or three cycles. Thus a plot of T versus N (the number of the cycle) consists of two ''plateaus.'' The first plateau, with the smaller T, yields a bulk modulus that agrees reasonably well with the intermediate value Eq. (2). Also, the relaxation time τ of these cycles is in reasonable agreement with Eq. (3). The second plateau, with the longer T, yields a bulk modulus in good agreement with the isothermal value

$$K_i=PZ. \tag{8}$$

The relaxation time of these oscillations is longer than τ_m (as one would expect for isothermal oscillations), but it was not possible to obtain reliable values because of the small amplitudes of the oscillations studied. The plot of T versus N showed a further feature, namely, an initial ''lip'' consisting of the first one or two cycles with a period slightly lower than that of the first plateau: these gave a bulk modulus close to the adiabatic value Eq. (6). (We remark that for air the resolution of this ''lip'' is near the limit of our experimental accuracy in the measurement of T.) For the smallest volumes of gas (the highest frequencies) we were unable to detect the second plateau before the amplitude decreased so much that the signal became distorted by noise, or the motion had ceased [1].

These results, showing that for a given volume of air the oscillations undergo several changes as their amplitude decreases due to damping, suggested the following interpretation: A transient, adiabatic oscillation is followed by several intermediate oscillations until, after the amplitude decreases sufficiently, there is a transition (lasting two or three cycles) to isothermal oscillations which persist until the motion ceases [1].

Because of the unexpected and incomplete nature of some of these results, and because they were obtained for just one gas, we have undertaken a further, more detailed, study. This study was motivated by the following questions:

(i) Are similar results found in other gases, in particular, the monatomic and polyatomic gases?

(ii) Can the sensitivity of the measurements be improved sufficiently to obtain accurate values of the relaxation time in the ''isothermal tail'' of the trace of $x(t)$ versus t? Such values are of interest because the relaxation time is more sensitive to the presence of thermal gradients in the oscillating gas than is the bulk modulus (see Ref. [1] and Secs. IV and V).

(iii) Equations (3) and (5) for the relaxation time enable one to make certain predictions regarding the damping of intermediate oscillations in various gases (for given values of the experimental parameters m, P, and A). In particular, at small volumes, the second term on the right-hand side of Eq. (3) is larger than the first term (see Secs. IV and V): Then, for example, a gas with a large thermal diffusivity κ, and a value of γ not too close to unity, should have large damping compared with a gas with a value of γ close to unity, and a κ that is not too large [see Eqs. (3) and (5)]. Thus from tables of κ and γ (see Appendix A), one can select gases which are in the ''high damping'' or ''low damping'' limits.

In the work reported here we have studied twelve gases: five monatomic gases (He, Ne, Ar, Kr, Xe), a diatomic gas (N_2), and six polyatomic gases (CO_2, N_2O, CHF_3, CCl_2F_2, C_2ClF_5, and SF_6) at room temperature and pressure. (The purity of these gases was in excess of 99.9%.) In Sec. II we give a brief discussion of our experimental procedure and present some representative traces of $x(t)$ for three gases, which exemplify the cases of low, medium, and high damping. Detailed results obtained from an analysis of approximately 700 traces measured for the above twelve gases are presented in Sec. III (the bulk moduli) and in Sec. IV (the relaxation times). These results are compared with theory and discussed in Section V.

II. EXPERIMENTAL PROCEDURE AND RESULTS

The apparatus was the same as that in Ref. [1] apart from two modifications: (1) Contamination of the gas in the aspirator by any exchange with air past the oscillating ball was prevented by inverting a glass cup over the open end of the tube, and continuously flushing this cup with the gas being used. (2) A pulsed magnetic field was used to induce the oscillation of the ball by discharging a capacitor through a coil mounted coaxially with the tube and located at the equilibrium position of the ball. The magnitude of the displace-

ment was controlled by adjusting the voltage applied to the capacitor.

The main obstacle to obtaining good traces at small amplitudes is mechanical noise associated with the motion of the ball in the tube. To reduce this noise it is essential that the ball and tube be clean, and that they contain no scratches or rough patches. Even then, the quality of traces at small amplitudes tends to be unsatisfactory for accurate measurements. The cause of this difficulty was found to be the filler liquid (water or vacuum pump oil) in the aspirator: after a time, small amounts of this liquid condense on the surface of the ball and the inside of the tube. When using vacuum pump oil, this condensation required that the apparatus be disassembled and cleaned. Because recontamination could occur relatively quickly, we abandoned the use of oil as a filler.

In the case of water, the ball and the tube can be dried, without disassembling the apparatus, by gently heating the tube with a hot-air blower along a length of about 5 cm on either side of the equilibrium position of the ball for a few minutes, and then allowing the tube to cool to room temperature before resuming measurements. This simple technique usually allows one to complete a run, lasting 10 h or more, on a given gas and to obtain good quality traces even for small oscillations (see below). The results reported here were obtained using water as a filler.

For each gas, we adopted the following procedure. The aspirator was filled up to the stopper with distilled water. Then a carefully measured volume of water was tapped out and the aspirator and tube were flushed with the gas being used. After the flushing was complete, the ball was given a displacement of about 6 cm and the desired traces were recorded on an xy plotter (see Ref. [1]). Then the volume of gas was increased by tapping out more water and the above process repeated. The smallest volume for which a reliable trace could be obtained was about 0.12 l.

In practice, it was convenient to use two sets of volume increments for each gas. The reason is that for determining the bulk moduli one uses Eq. (1) and a widely spaced set of volumes (about 20) between 0.12 and 22.94 l is suitable (see Sec. III). However, for the relaxation times one wishes to test Eq. (3), and an appropriately spaced set of traces (again about 20) for volumes between 0.12 and about 7 l is more suitable (see Sec. IV). Also, many of the traces had to be measured twice: once for the initial oscillations and a second, amplified trace for the ''tail'' of the oscillations. It turned out that about 60 traces were recorded for each gas. The method for measuring the period of each cycle was the same as that in Ref. [1]. The trace of $x(t)$ was captured on a digital oscilloscope and, using the ''x-enlargement'' feature of the oscilloscope, accurate values for the periods were obtained. See Ref. [1] for more details.

We present some typical traces for various volumes of three gases (N_2, He, and CCl_2F_2) in Figs. 1 and 2. These gases have been chosen because they cover a wide range of damping and the traces give a good indication of the variety of behavior observed in our experiments. We mention some general features:

(i) Plots of the period T versus the number of the cycle N obtained from traces such as those in Figs. 1 and 2 are shown in Figs. 3–5. These plots confirm the results found previously for air [1], namely, a single plateau at the smaller volumes of gas and two plateaus at the larger volumes. The second plateau is associated with the oscillations in the tail of the trace: the onset of these plateaus is indicated by arrows in Figs. 2(a), 2(b), and 2(c).

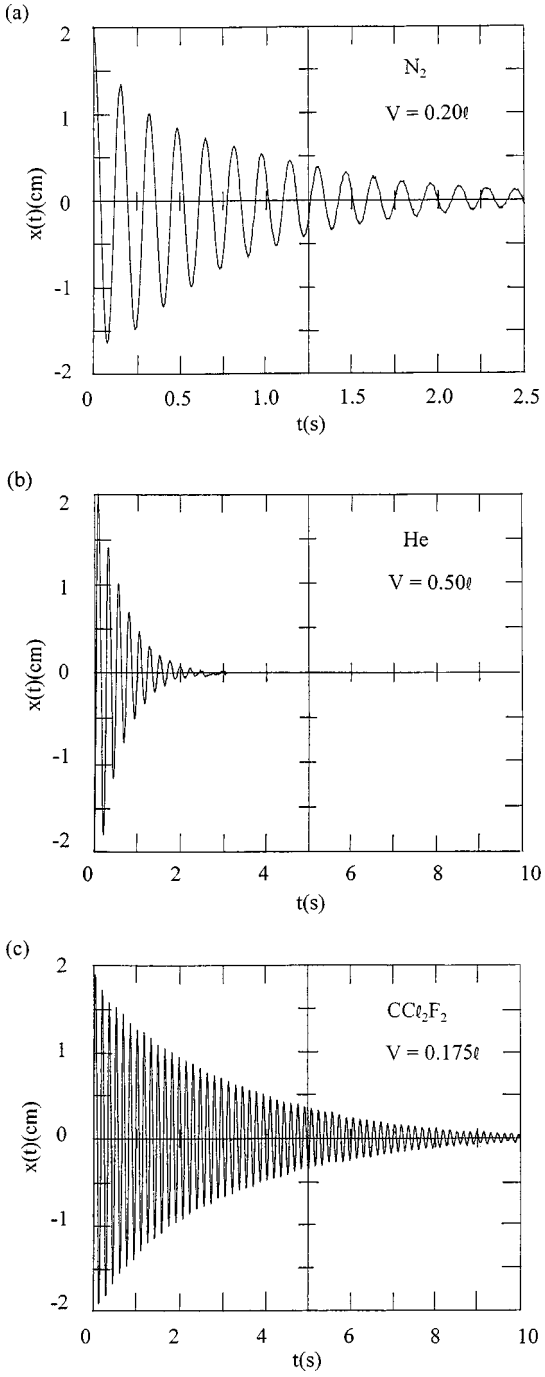

FIG. 1. (a) Oscilloscope trace for the position x of the steel ball vs t, for a volume $V=0.20$ l of N_2. The first 15 cycles are shown. (b) As in (a) but for a volume $V=0.50$ l of He. The jitter at the end of the trace is due to noise inherent in our xy recorder. (c) As in (a) but for a volume $V=0.175$ l of CCl_2F_2. Note the slight beatlike property of the oscillations.

(ii) The amplitudes in the tail increase as the volume is increased (see Sec. V). Consequently, for a given initial displacement, the number of cycles in the first plateau decreases

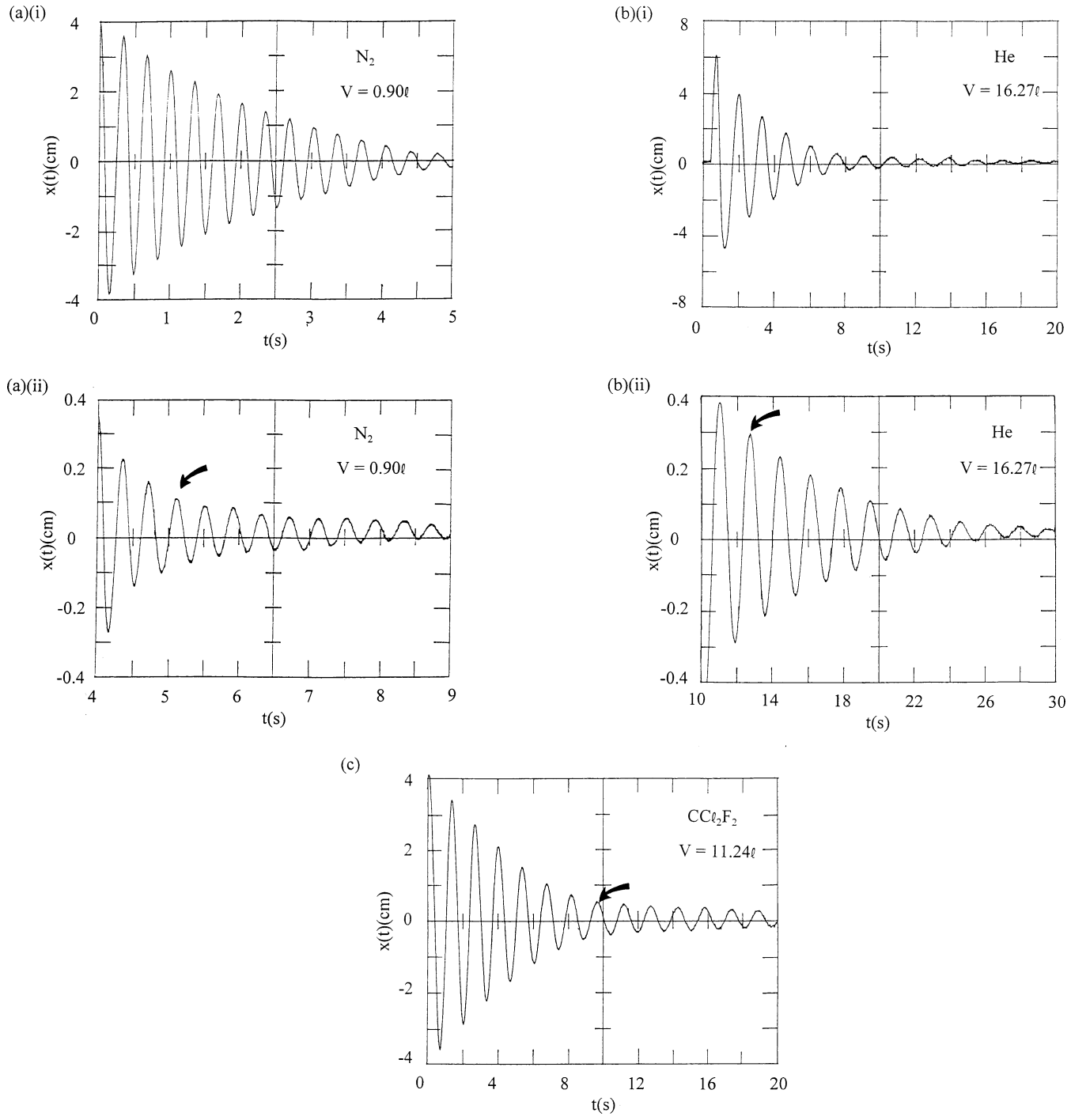

FIG. 2. (a) (i) As in Fig. 1(a) but for a volume $V = 0.90$ l of N_2. The first 14 cycles are shown. (ii) An amplified tail, showing cycles 12–23. The arrow indicates the first peak in the tail. (b) (i) As in Fig. 1(a) but for a volume $V = 16.27$ l of He. The first 13 cycles are shown. (ii) An amplified tail, showing cycles 8–18. The arrow indicates the first peak in the tail. (c) As in Fig. 1(a) but for a volume $V = 11.24$ l of CCl_2F_2. The arrow indicates the first peak in the tail.

as the volume increases (Figs. 3–5): at larger volumes the tail starts almost at the beginning of the trace.

(iii) For a given volume of gas, the number of cycles in the first plateau depends on the initial displacement; the number of cycles in the second plateau does not. The amplitude at the start of the second plateau does not depend on the initial amplitude.

(iv) At the smaller volumes, the damping of the first set of oscillations with constant period (those in the first plateau) varies strongly with the type of gas [compare Figs. 1(a), 1(b), and 1(c)]. For these oscillations, He has large damping, CCl_2F_2 has low damping, and N_2 is intermediate between the two (see Sec. IV).

(v) The damping in the tails of the oscillations is less than that of the initial oscillations, particularly for the larger volumes of gas (see Fig. 2 and Sec. IV). Also, at large volumes the gases have about the same damping in the tails (Sec. IV).

A detailed analysis and interpretation of the results ob-

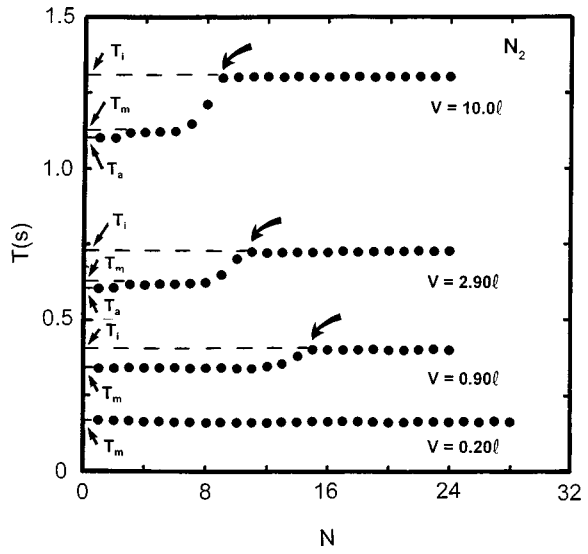

FIG. 3. The measured period T of a cycle vs the number N of that cycle for various volumes of N_2. The data were obtained from traces such as those in Figs. 1 and 2, as described in the text. The arrows indicate the first cycle in the tail. The manner in which the periods T_a, T_m, and T_i are obtained is shown.

tained from approximately 700 traces is given in the following sections.

III. BULK MODULI

The bulk moduli are determined from the measured periods using the procedure of Ref. [1]: Equation (1) is rewritten in terms of the volume of water in the aspirator $V_w = V_0 - V$ where V_0 is the volume of the empty aspirator plus the volume of the tube up to the equilibrium position of the ball) as

$$T^2 = \frac{4\pi^2 m}{KA^2}(V_0 - V_w). \tag{9}$$

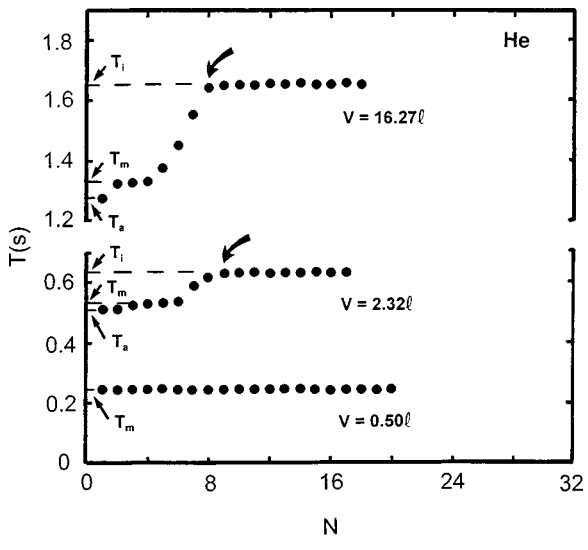

FIG. 4. As in Fig. 3 but for He.

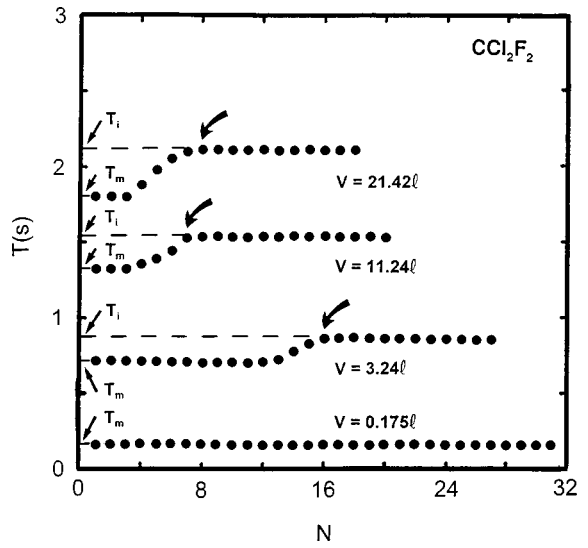

FIG. 5. As in Fig. 3 but for CCl_2F_2.

According to Eq. (9), for oscillations of a given type, a plot of T^2 versus V_w should yield a straight line with slope $-4\pi^2 m/KA^2$ and intercept V_0. In this section we present our experimental results for the bulk moduli, together with theoretical values for adiabatic, intermediate, and isothermal oscillations. The results are discussed in Sec. V.

A. Monatomic gases

Plots of T^2 versus V_w for He are shown in Fig. 6. The straight lines are obtained from least-mean-squares fits to the data. The points labeled T_a^2 are from the measured periods of the initial one (or two) cycles of the traces, such as the values T_a in Fig. 4. The points labeled T_m^2 are from the periods of the first plateau, such as the values T_m in Fig. 4. The points labeled T_i^2 are from the periods of the second plateau, such as the values T_i in Fig. 4. We remark that in He values of T_m

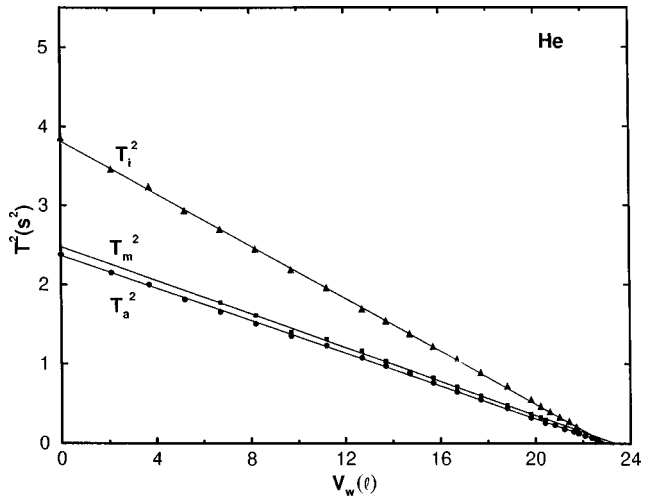

FIG. 6. The squares of the periods T_a, T_m, and T_i vs the volume of water in the aspirator, for He. The values of T_a, T_m, and T_i were obtained from plots such as Fig. 4. The straight lines are least-mean-squares fits to the data, and the intercepts and slopes are given in Table I.

TABLE I. Values of the intercepts and slopes for five monatomic gases obtained from least mean-squares fits such as those in Fig. 6. Values of the equilibrium temperature and pressure of each gas are also given.

Gas	t (C)	P (Pa)	V_{0a} (l)	V_{0m} (l)	V_{0i} (l)	$\frac{dT_a^2}{dV_w}$ ($s^2\,l^{-1}$)	$\frac{dT_m^2}{dV_w}$ ($s^2\,l^{-1}$)	$\frac{dT_i^2}{dV_w}$ ($s^2\,l^{-1}$)
He	21	95 660	23.04	23.36	23.00	−0.1026	−0.1060	−0.1657
Ne	22	92 820	23.08	23.04	22.95	−0.1066	−0.1096	−0.1656
Ar	18	93 400	22.92	22.90	22.70	−0.1030	−0.1060	−0.1665
Kr	24	92 950	22.93	22.98	22.63	−0.1058	−0.1077	−0.1622
Xe	23	92 320	23.00	22.96	22.98	−0.1071	−0.1087	−0.1574

could not be obtained for the larger volumes of gas ($V_w \lesssim 6$ l) because the initial plateau cannot be discerned at these volumes. Also, for smaller volumes of gas ($V_w \gtrsim 21$ l) the difference between T_a and T_m could not be resolved in our measurements (see Fig. 4). Values of the intercepts and slopes obtained from Fig. 6 are given in Table I. The values of V_0 obtained from the respective intercepts are all close to the measured value $V_0 = 22.94$ l. In Table II we present values of the bulk moduli divided by the equilibrium pressure K/P deduced from the measured slopes dT^2/dV_w with the aid of Eq. (9) and using $m = 16.5 \times 10^{-3}$ kg and $A = 2.011 \times 10^{-4}$ m^2.

The theoretical values of the bulk moduli in Table II were obtained from Eqs. (2) and (6)–(8) using the parameters listed in Appendix A. Note that we have neglected the effect of water vapor in the gas on the value of γ because this effect is small [1], and that we have rounded off all values of the bulk moduli to 3 significant figures. In calculating the ratio a/R in Eq. (2) we use Eq. (1), with $V = \frac{4}{3}\pi R^3$, in Eq. (4) to write

$$\frac{a}{R} = \left(\frac{\gamma\kappa}{\pi}\right)^{1/2}\left(\frac{16\pi^3 m}{3\gamma P A^2}\right)^{1/3} T^{-1/6}. \tag{10}$$

The factor $T^{-1/6}$ in Eq. (10) is within 12% of 1 $s^{-1/6}$ for the values of T for which we measure a difference between T_a and T_m (i.e., for 2 s $\gtrsim T \gtrsim$ 0.5 s): in the calculations of K_m/P in Table II we have set this factor equal to unity. Results obtained in a similar manner for four other monatomic gases are also given in Tables I and II.

TABLE II. Experimental values of the bulk moduli for five monatomic gases obtained from Eq. (9) using the data in Table I. The theoretical values are obtained from Eqs. (2), (6), (7), and (8) as described in the text.

	K_a/P		K_m/P		K_i/P	
Gas	Expt.	Theory	Expt.	Theory	Expt.	Theory
He	1.64	1.63	1.59	1.56	1.02	1.00
Ne	1.63	1.64	1.58	1.60	1.05	1.00
Ar	1.67	1.67	1.63	1.64	1.04	1.00
Kr	1.64	1.67	1.61	1.65	1.07	1.00
Xe	1.63	1.65	1.61	1.63	1.10	1.00

B. Nitrogen

Plots of T_a^2, T_m^2, and T_i^2 versus V_w for N_2 are shown in Fig. 7, and the results obtained from these are given in Tables III and IV. In the latter table, theoretical values of the bulk moduli are also presented.

C. Polyatomic gases

Our measurements on polyatomic gases yield unexpected values for the bulk moduli K_i of the oscillations in the tail of $x(t)$. As a result, we decided to make a detailed study of several gases of increasing polyatomicity. To illustrate the measurements, we present in Figs. 8 and 9 plots of T^2 versus V_w for two gases, CO_2 and C_2ClF_5. A noteworthy feature of the plots of T_i^2 versus V_w in these figures is the unexpectedly large values of the periods, which results in smaller than expected values of the bulk moduli K_i: This feature is present in all the polyatomic gases we have studied (see Table VI and Sec. V). The results of our measurements on six polyatomic gases are presented in Tables V and VI, and theoretical values of the bulk moduli are included in Table VI. We remark that for the four most polyatomic gases (CHF_3, CCl_2F_2, SF_6, and C_2ClF_5) we were unable to distinguish any difference in the period of the initial oscillations T_a and that of the first plateau T_m. For this reason, values corresponding to T_a are not given in Fig. 9 or in Tables V and VI. We note that the effect of molecular interactions on the bulk moduli K_a, K_m, and K_i has been included in the

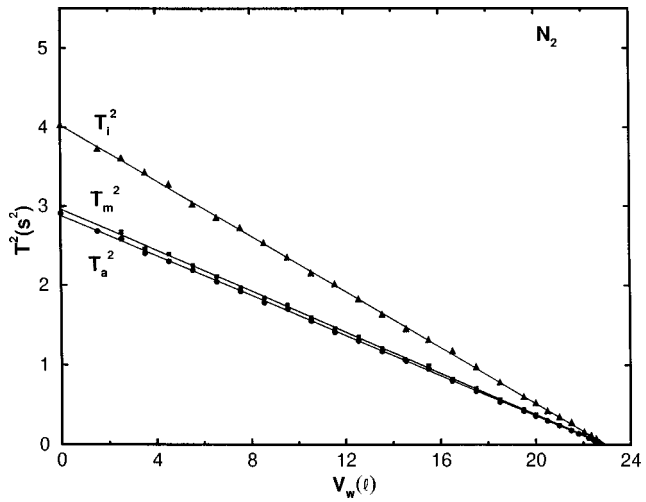

FIG. 7. As in Fig. 6 but for N_2. The intercepts and slopes are given in Table III.

TABLE III. As in Table I, but for N_2.

Gas	t (C)	P (Pa)	V_{0a} (l)	V_{0m} (l)	V_{0i} (l)	$\frac{dT_a^2}{dV_w}$ ($s^2\,l^{-1}$)	$\frac{dT_m^2}{dV_w}$ ($s^2\,l^{-1}$)	$\frac{dT_i^2}{dV_w}$ ($s^2\,l^{-1}$)
N_2	24	92 300	22.90	22.95	22.97	−0.1258	−0.1290	−0.1751

theoretical values in Tables II, IV, and VI by means of the compressibility factor Z in Eqs. (6) and (8). Numerical values of this factor for our gases are listed in Appendix A: the effect of interactions under the conditions of our experiment is usually small, but it can reduce the bulk modulus by about 3% in the polyatomic gases (Appendix A).

IV. RELAXATION TIMES

The relaxation times are determined from the ratio of successive peak-to-peak displacements x_n/x_{n+1} and the measured periods T, using the relation

$$\tau = \frac{T}{\ln x_n/x_{n+1}} \tag{11}$$

for a damped oscillator. In this section we present results for (i) the relaxation times τ_m of the intermediate oscillations (those with period T_m, see Sec. II) and (ii) the relaxation times τ_i of the oscillations in the tail of $x(t)$ (those with period T_i, see Sec. II).

A. The relaxation times τ_m

For each volume of a given gas, the value of τ_m was obtained as an average of the values given by Eq. (11) for all the cycles with period T_m. The maximum variation of the values of τ_m from the mean was about 20%. This variation is associated with a slight beatlike property of the traces of $x(t)$: see, for example, Fig. 1(c). To compare the measured values with Eq. (3), we plot $1/\tau_m$ versus $T_m^{-7/6}$. This is done in Fig. 10 for the monatomic gases and in Fig. 11 for N_2 and the polyatomic gases. The straight lines in these figures are least-mean-squares fits to the data. From these straight lines we obtain, for each gas, values of the slope D and the intercept $1/\tau_0$ listed in Table VII. Included in this table are theoretical values of D calculated from Eq. (5) and using the parameters given in Appendix A. Note that the volumes of gas used in obtaining the data in Figs. 10 and 11 are small (see Fig. 12).

B. The relaxation times τ_i

For our purposes it is helpful to compare the values of τ_m and τ_i by including the latter in a plot of $1/\tau_m$ versus $T_m^{-7/6}$. This is done in Fig. 12 for three gases He, N_2, and N_2O. All the gases we studied yielded results similar to those in Fig. 12. Specifically, for a given volume of gas, τ_i is always longer than τ_m. This is particularly the case as the volume of gas (and hence the period of oscillation) is increased (see Fig. 12). Further discussion of these results is given in the next section.

TABLE IV. As in Table II, but for N_2.

	K_a/P		K_m/P		K_i/P	
Gas	Expt.	Theory	Expt.	Theory	Expt.	Theory
N_2	1.39	1.40	1.35	1.38	1.00	1.00

V. DISCUSSION

We summarize the picture that is suggested by our experiments:

(1) There is evidence for an initial, transient adiabatic part to the oscillations. This transient lasts for the first one or two cycles, which have a slightly lower period (T_a) than that of the prolonged set of cycles with constant period (T_m) that follow (see, for example, the ''lips'' in Figs. 3 and 4). From the periods T_a we obtain bulk moduli K_a that are in reasonable agreement with theoretical values for adiabatic oscillations (see Tables II, IV, and VI, and Ref. [1]). However, we make two comments on this result: (i) We are unable to support the conclusion by measuring also a relaxation time τ_a, because there are too few adiabatic oscillations. (ii) Measurement of a difference between T_a and T_m is close to the limit of our experimental accuracy for time measurement and, in fact, in the polyatomic gases with low γ we are unable to measure such a difference (see Secs. II and IV).

By contrast, the intermediate oscillations (those with period T_m) can be studied in more detail and with greater accuracy. Measurements of both the bulk moduli K_m and the relaxation times τ_m are in reasonable agreement with a model that takes into account the departure from adiabaticity due to heat flows into and out of the gas (see Tables II, IV, VI, and VII). The effect on the bulk modulus is to lower it,

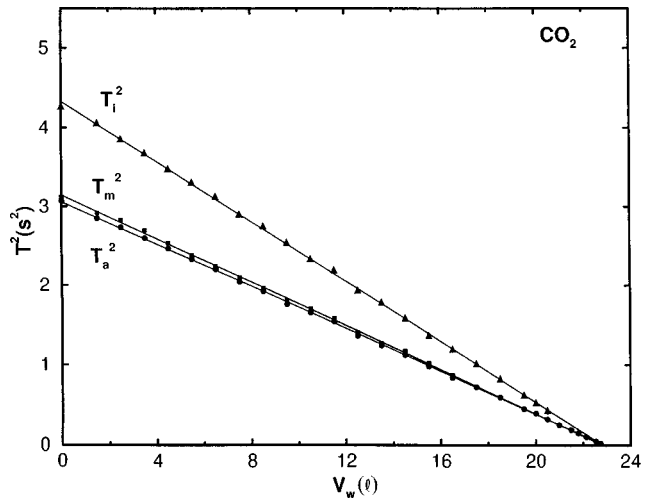

FIG. 8. As in Fig. 6 but for CO_2. The intercepts and slopes are given in Table V.

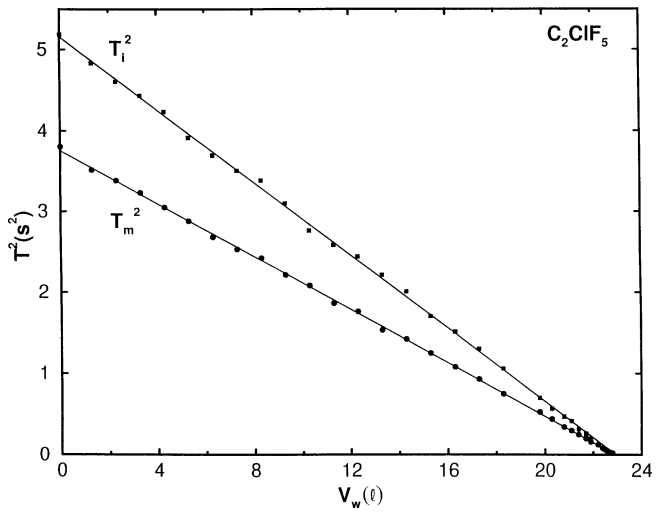

FIG. 9. As in Fig. 6 but for C_2ClF_5. The intercepts and slopes are given in Table V.

typically by a few percent, or less. The effect on the relaxation time can be more pronounced, particularly for the smaller volumes of gas: if the contribution of thermal gradients to the dissipation were absent, the second term on the right-hand side of Eq. (3) would be zero, and plots such as Figs. 10 and 11 would be horizontal lines drawn through the intercepts on the $1/\tau$ axis. The dependence of $1/\tau$ on $T^{-7/6}$ in Eq. (3) is in reasonable agreement with the measured values in Figs. 10 and 11. The prediction that gases such as He and Ne are in the high damping limit, whereas polyatomic, low-γ gases such as SF_6, CCl_2F_2, and C_2ClF_5 are in the low damping limit, is also borne out by experiment (see Table VII). We conclude that the identification and properties of the intermediate oscillations have good experimental support. (With regard to the comparison of theoretical and experimental values of the slopes D in Table VII, we remind the reader that the former are for a spherical aspirator whereas the shape of our aspirator, for the volumes used in obtaining the experimental values, is conical. The error introduced by this disparity is unknown.)

(3) Equations (3) and (5) can be used to estimate the damping of intermediate oscillations for other gases. For example, for H_2 ($\gamma=1.40$ and $\kappa=15.4\times10^{-5}$ m^2 s^{-1}) the value of D is about 0.7 that for He, or approximately $0.37s^{1/6}$. Thus H_2 should also exhibit large damping due to heat flows. It is interesting to ask which gas has the lowest damping associated with heat flow. From the tabulated information available to us, this is C_4F_8 ($\gamma=1.057$ and $\kappa=0.15\times10^{-5}$ m^2 s^{-1}), for which D is about 2.2 times smaller than the value of the gas with lowest damping in our experiments (C_2ClF_5, see Table VII). It would be interesting to check this prediction.

(4) Next, we discuss the oscillations in the tail of $x(t)$ (the oscillations with period T_i that make up the second plateau in plots such as Figs. 3–5). These we also studied in detail, measuring both the corresponding bulk moduli K_i and the relaxation times τ_i. For the monatomic and diatomic gases, the measured values of K_i are close to the values for isothermal oscillations, except for Kr and Xe where they are a little high (see Table II). This indication of isothermal oscillations is supported by measurements of τ_i: If the oscillations are isothermal, the damping should be mainly due to friction in the tube. That is, $\tau\approx\tau_0$, the inverse of the first term in Eq. (3). The plots in Fig. 12, where τ_i and τ_m are compared, show that for the larger volumes of gas ($V\gtrsim1$ l in the case of N_2) this is, in fact, so. (For the largest volumes of gas, the values of $1/\tau_i$ are actually as much as 50% below the intercepts $1/\tau_0$ obtained from the plots of $1/\tau_m$: the reason for this is not clear. Also, for the smaller volumes of gas, the values of $1/\tau_i$ in Fig. 12 lie above the intercepts, but still below $1/\tau_m$: this suggests that at these volumes there is some residual dissipation due to temperature gradients. It should be recalled that the values of K_i are obtained using volumes of gas that are mostly larger than 1 l: see Figs. 6–9.) We conclude that for the monatomic and diatomic gases we have studied, our measurements of the bulk moduli and relaxation times indicate the presence of (approximately) isothermal oscillations in the tails of $x(t)$.

(5) For the six polyatomic gases we have studied, the results provide an unexpected twist. The measurements of τ_i still indicate the absence of a contribution from thermal gradients at the larger volumes of gas [see Fig. 12(c) for N_2O; similar results are obtained for the other polyatomic gases]. However, the values of K_i are all lower than the theoretical values, and the disparity increases as the degree of polyatomicity increases (see Table VI). The reason for these differences is not clear: they are not due to molecular interactions because (i) these are included in the theoretical values in Table VI and (ii) the thermodynamic identity [7] $K_a/K_i=\gamma$ would require the same effect on the values of K_a and K_m [which is proportional to K_a in Eq. (2)], and this is not evident in our measurements of K_a and K_m in Table VI. We emphasize that the measured values of K_i in Table VI are

TABLE V. As in Table I, but for polyatomic gases.

Gas	t (C)	P (Pa)	V_{0a} (l)	V_{0m} (l)	V_{0i} (l)	$\frac{dT_a^2}{dV_w}$ (s^2 l^{-1})	$\frac{dT_m^2}{dV_w}$ (s^2 l^{-1})	$\frac{dT_i^2}{dV_w}$ (s^2 l^{-1})
CO_2	23	92 200	22.89	22.83	22.82	−0.1336	−0.1377	−0.1896
N_2O	25	92 030	22.94	22.98	22.84	−0.1384	−0.1408	−0.1987
CHF_3	23	92 050		22.94	22.96		−0.1507	−0.2063
CCl_2F_2	16	93 980		22.90	23.02		−0.1566	−0.2077
SF_6	22	94 600		23.01	23.09		−0.1600	−0.2143
C_2ClF_5	17	93 730		22.91	22.94		−0.1635	−0.2244

TABLE VI. As in Table II, but for polyatomic gases.

	K_a/P		K_m/P		K_i/P	
Gas	Expt.	Theory	Expt.	Theory	Expt.	Theory
CO_2	1.31	1.31	1.27	1.30	0.92	1.00
N_2O	1.27	1.29	1.24	1.28	0.88	0.99
CHF_3		1.18	1.16	1.18	0.85	0.99
CCl_2F_2		1.12	1.09	1.12	0.83	0.98
SF_6		1.08	1.06	1.08	0.80	0.99
C_2ClF_5		1.07	1.05	1.07	0.77	0.97

reproducible and they are not affected by the presence of liquid in the aspirator. One can make an independent check by using a dry empty aspirator, filling it successively with various gases, and measuring the periods T_i of each. These values correspond accurately and reproducibly to the intercepts on the T_i^2 axis in plots such as Figs. 6–9. [Note how these intercepts increase as the gases become more polyatomic: the bulk moduli are inversely proportional to these intercepts, see Eq. (9).] As a further check of the values of K_i, we have repeated our measurements using a larger, plastic aspirator (total volume $\sim$56 l): The values of K_i obtained from the plots of T_i^2 versus V_w are in good agreement with those in Table II, IV, and VI.

(6) The frictional force associated with motion of the ball in the tube is $F_0=\beta_0 v$ where $\beta_0=m/2\tau_0$. Values of β_0 can be obtained from our measurements of τ_0. Consider, for example, N_2. From Fig. 12 we have $\tau_0\approx 6$ s from the intercept obtained using measurements of τ_m and $\tau_0\approx 12$ s by extrapolating the measurements of τ_i to zero frequency. These give $\beta_0\approx 1.4\times 10^{-3}$ N m^{-1} s and $\beta_0\approx 0.7\times 10^{-3}$ N m^{-1} s, respectively. By comparison, the frictional force given by the Stokes formula for motion of the ball in an infinite gas is $F_\infty=\beta_\infty v$ where $\beta_\infty=6\pi a\eta$ and a is the radius of the ball. For our ball ($a=8$ mm) in N_2 ($\eta\approx 20\times 10^{-6}$ Pa s), $\beta_\infty\approx 3\times 10^{-6}$ N m^{-1} s. Thus

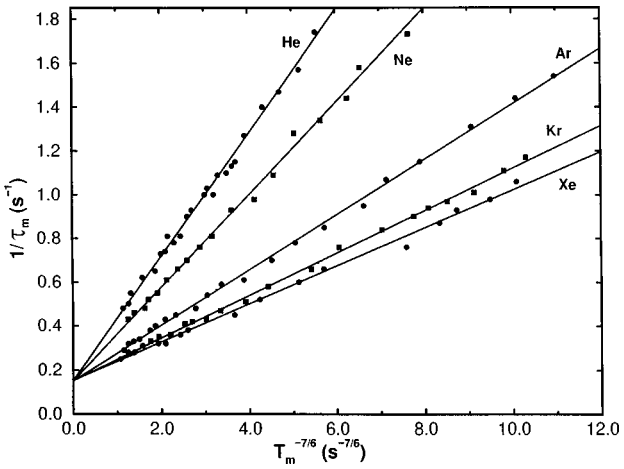

FIG. 10. A test of Eq. (3) for monatomic gases: a plot of $1/\tau_m$ versus $T_m^{-7/6}$. The values of τ_m were obtained as described in the text. The straight lines are least-mean-squares fits to the data, and the intercepts and slopes are given in Table VII.

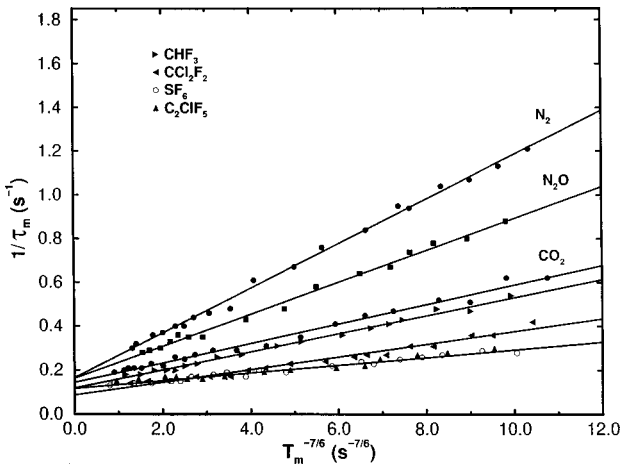

FIG. 11. As in Fig. 10 but for diatomic and polyatomic gases. The fit for C_2ClF_5 is very close to that for SF_6, and has not been drawn for clarity.

$$F_0/F_\infty\approx 460 \tag{12}$$

using the measurements of τ_m, and

$$F_0/F_\infty\approx 230 \tag{13}$$

using the measurements of τ_i. An approximate calculation of this ratio yields (see Appendix B)

$$F_0/F_\infty\approx C\sqrt{2a/\epsilon}, \tag{14}$$

where C is of order unity, ϵ is the clearance between the tube and the ball, and we have assumed that $\epsilon\ll a$. In our experiment, $\epsilon\approx 0.005$ mm and hence Eq. (14) gives $F_0/F_\infty\approx 60$.

TABLE VII. Values of the slopes (D) and the intercepts ($1/\tau_0$) in Eq. (3) obtained from the least-mean-squares fits in Figs. 10 and 11. The theoretical values of D are calculated using Eq. (5).

	$1/\tau_0$ (s^{-1})	$D(10^{-2}$ s$^{1/6})$	
Gas	Expt.	Expt.	Theory
He	0.16	28	53
Ne	0.14	21	32
Ar	0.15	13	19
Kr	0.15	10	14
Xe	0.15	8.7	11
N_2	0.16	10	14
CO_2	0.14	4.4	7.9
N_2O	0.16	7.3	7.3
CHF_3	0.12	4.1	4.4
CCl_2F_2	0.12	2.9	2.1
SF_6	0.12	1.8	1.5
C_2ClF_5	0.086	1.8	1.4

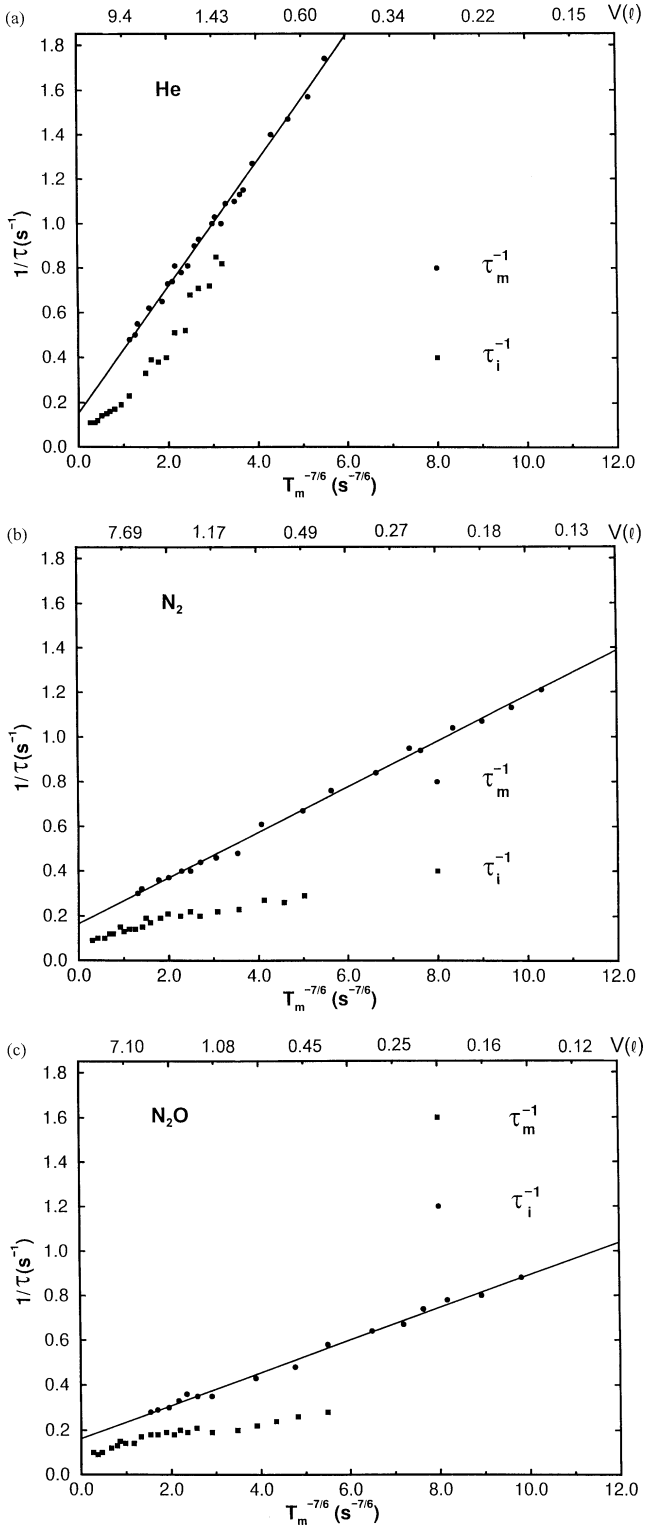

FIG. 12. (a) Comparison of τ_i and τ_m for He on a plot of $1/\tau$ versus $T_m^{-7/6}$. The data points for $1/\tau_m$ and the straight-line fit are the same as for He in Fig. 10. Values of the volume of gas are indicated on the upper horizontal axis. (b) As in (a) but for N_2. (c) As in (a) but for N_2O.

We note that according to Eq. (B2), $1/\tau_0$ is proportional to the viscosity of the gas. For our gases, the viscosity varies between about 15 μPa s and 30 μPa s. However, our measurements of $1/\tau_0$ yield mostly quite similar values (Table VII) and are probably not sufficiently accurate to test for any dependence on viscosity.

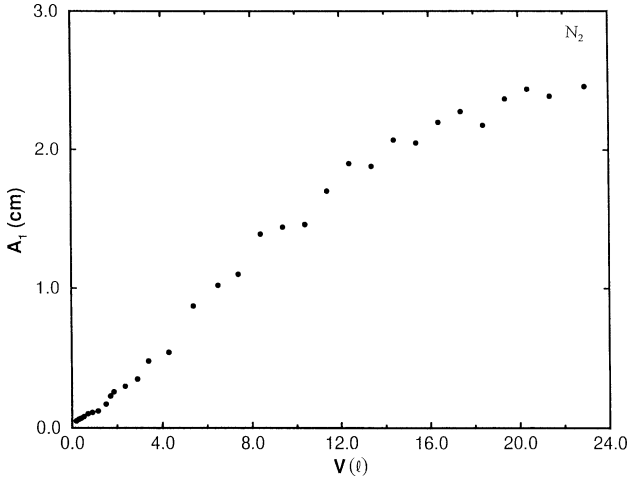

FIG. 13. Plot of the amplitude of the first peak (or trough) A_1 in the tail vs the volume of gas V for N_2.

(7) Another measurable property of the tails is their amplitudes. These amplitudes increase with the volume of gas (see Figs. 1 and 2). To quantify this, we have measured the amplitude of the first oscillation in the tail (A_1) as a function of the volume. (A_1 is the amplitude of the first peak, or trough, of the first cycle with period T_i: for example, the peaks are indicated with arrows in Fig. 2. Frequently there is uncertainty in identifying this peak, or trough, among two or three neighboring candidates, and this produces an uncertainty of some 20% in the values of A_1.) In our experiments the amplitudes increase by about a factor 50 over the range of volumes used; see Fig. 13 where results for N_2 are presented.

It may seem surprising that in our experiments isothermal oscillations are more easily established as the volume of gas is increased (Fig. 13). After all, the distance scale for the conduction of heat out of and into the gas increases with the volume. To discuss this point it is helpful to recall an analysis first presented by Stokes to determine whether sound waves in gases propagate under adiabatic or isothermal conditions [8]. Stokes noted that the time available (the period of oscillation T) for heat to be transported from a region of compression in the wave to neighboring regions of rarefaction scales inversely with the frequency ν:

$$T \sim 1/\nu. \tag{15}$$

He therefore concluded that if the frequency is lowered, the oscillations should become isothermal. Conversely, at high frequency, where T becomes small, the oscillations should be adiabatic.

It was later recognized that, at least for an infinite gas, this argument is incomplete and the conclusion is erroneous [8]. It must be taken into account that the distance R that the heat has to be conducted is of the order of the wavelength, and hence it scales inversely with the frequency

$$R \sim 1/\nu. \tag{16}$$

The scalings (15) and (16) represent two competing influences: A detailed analysis shows that the oscillations are adiabatic in the low-frequency limit and they become isothermal in the high-frequency limit [9], which is the opposite to Stokes' conclusion. Here ''low'' and ''high'' are relative to a characteristic frequency $\sim 10^9$ Hz for gases under standard conditions [9].

In our experiments on oscillations in confined gases the situation is different: For a given volume of gas, the wavelength of the oscillation is much greater than the dimensions of the container [1]. [For example, for 0.2 l of N_2, Eq. (1) and Table III show that $\nu \approx 6.3$ Hz and hence $\lambda \approx 52$ m. If the gas occupies a sphere, the radius is $\approx 3.6 \times 10^{-2}$ m and hence (radius)/(wavelength) $\approx 7 \times 10^{-4}$.] Consequently, instead of Eq. (16) one has for the distance heat has to be conducted

$$R \sim \text{dimension of the container.} \tag{17}$$

The appropriate distance to be used in Eq. (17) depends on the geometry of the container. For example, for a sphere it is the radius, and so $R \sim V^{1/3}$. Also, according to Eq. (1) $\nu \sim V^{-1/2}$. Hence

$$R \sim 1/\nu^{2/3}. \tag{18}$$

The result (18) applies also to conical containers of fixed angle. According to Eq. (18)

$$R/\lambda \sim \nu^{1/3}$$

decreases as the frequency decreases (i.e., as the volume increases). For example, for 23 l of N_2, $\nu \approx 0.6$ Hz and $R/\lambda \approx 3 \times 10^{-4}$ compared with a ratio 7×10^{-4} for 0.2 l of N_2. Thus in our experiments the ratio R/λ is small at the smallest volumes of gas, and it decreases further as the volume of gas is increased. Perhaps it is this feature that makes it easier to detect the isothermal tail at large volumes.

It is interesting to note that for a long, thin cylinder Eq. (17) is

$$R \sim (\text{diameter of the cylinder}),$$

which remains fixed if one increases the volume by increasing the length of the cylinder. In this case, one is dealing with just the scaling assumed by Stokes, namely, Eq. (15). One therefore expects that for such a cylinder isothermal conditions would be established more easily than for a sphere or cone of the same volume.

ACKNOWLEDGMENTS

We thank our colleagues, Rober Raab and Assen Ilchev, for helpful discussions; Sandy Diederichs, Nithaya Chetty, Guy Dewar, Allan Cullis, Johnny Wilsenach, and Karl Penzhorn for technical assistance; and the South African Foundation for Research and Development for financial support.

APPENDIX A

Table VIII below lists parameters used.

TABLE VIII. Values of parameters used in evaluating Eqs. (2), (4), (5), (6), (8), and (10) in the text.

Gas	C_p[a] ($J\ kg^{-1}\ C^{-1}$)	λ[b] ($10^{-2}\ W\ m^{-1}\ C^{-1}$)	κ[d] ($10^{-5}\ m^2\ s^{-1}$)	γ[a]	B[f] ($cm^3\ mol^{-1}$)	Z[g]
He	5196	14.7	18.1	1.63	12.0	1.0005
Ne	1030	4.78	6.1	1.64	11.3	1.0004
Ar	524.1	1.69	2.1	1.67	−16.7	0.9994
Kr	251.2	0.91	1.1	1.67	−52.0	0.9980
Xe	159.9	0.53	0.67	1.66	−136	0.9949
N_2	1037	2.53	2.3	1.40	−5.61	0.9998
CO_2	858.1	1.53	1.1	1.31	−126	0.9952
N_2O	878.2	1.48	1.0	1.30	−139	0.9948
CHF_3	736.7	1.54[c]	0.79	1.19[e]	−186	0.9930
CCl_2F_2	607.0	0.94	0.32	1.14	−416	0.9835
SF_6	666.6	1.37	0.36	1.09[e]	−287	0.9888
C_2ClF_5	686.5	1.05[c]	0.25	1.10	−717	0.9713

[a] *Matheson Gas Data Book*, 5th ed. (Matheson Gas Products, East Rutherford, New Jersey, 1971).

[b] *Matheson Gas Data Book*, and scaled to the appropriate temperature (see Tables I, III, V) using $\lambda \sim T^{1/2}$.

[c] R. W. Gallant, *Physical Properties of Hydrocarbons* (Gulf, Houston, 1968), Vol. 1.

[d] Calculated using $\kappa = \lambda/\rho C_\rho$ where $\rho (= MP/RT)$ is the density.

[e] Calculated using $\gamma = MC_p/(MC_p - R)$.

[f] J. H. Dymond and E. B. Smith, *The Virial Coefficients of Gases* (Clarendon Press, Oxford, 1969). We have extrapolated to 20 C.

[g] Calculated using $Z = 1 + B/\overline{V}$ and $\overline{V} = RT/P$ with the appropriate values of T and P.

APPENDIX B

The frictional force on a sphere of radius a moving with constant velocity v in an infinite fluid with viscosity η is given by (at low Reynolds number) Stokes's formula

$$F_\infty = 6\pi a\,\eta v. \tag{B1}$$

We consider the problem of a sphere moving along the axis of a long cylinder of radius a_c. Then Eq. (B1) is modified to

$$F_0 = 6\pi a\,\eta v\,\Delta \tag{B2}$$

where the factor Δ is a function of a/ϵ with $\epsilon = a_c - a$ the clearance between the cylinder and the sphere. For example, for small values of a/ϵ

$$\Delta \approx 1 + \frac{K}{1+\epsilon/a}, \tag{B3}$$

where $K \approx 2$ [10]. In our experiment $a/\epsilon \approx 1.6\times 10^3$ and we are therefore concerned with the opposite limit

$$a/\epsilon \gg 1, \tag{B4}$$

where $\Delta \to \infty$. In this appendix we estimate the factor Δ in the limit (B4).

We choose spherical coordinates attached to the sphere, with origin at the center of the sphere as shown in Fig. 14. The clearance at the position of the strip shown is $y = \epsilon + a(1-\sin\theta)$. We start by approximating the velocity gradient of the gas at the surface of the sphere by the value for a plane moving parallel to a second plane, namely

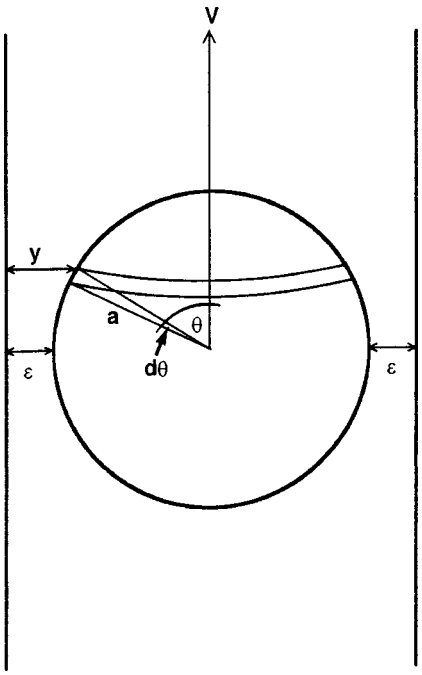

FIG. 14. Geometry for a sphere moving along the axis of a cylinder.

$$v/y. \tag{B5}$$

With this approximation, the frictional force on the sphere is given by

$$F_0 = 2\pi a^2 \eta v \int_0^\pi \frac{\sin^2\theta\, d\theta}{\epsilon + a(1-\sin\theta)}. \tag{B6}$$

In the limit (B4), most of the contribution to the above integral comes from a small region on either side of the equator ($\theta = \pi/2$): We can therefore set $\sin^2\theta = 1$ in the numerator of this integral (the error involved, for our value of a/ϵ, is about 4%). Thus we rewrite Eq. (B6) as

$$F_0 \approx 2\pi a\,\eta v \int_0^\pi \frac{d\theta}{1-(1+\epsilon/a)^{-1}\sin\theta}. \tag{B7}$$

The integral in Eq. (B7) is standard [11]: evaluated in the limit (B4) it is approximately $\pi\sqrt{2a/\epsilon}$. Thus the approximation (B5) and the limit (B4) yield the estimate

$$\Delta \approx \tfrac{1}{3}\,\pi\sqrt{2a/\epsilon}. \tag{B8}$$

(It is interesting to compare the dependence of the frictional force on $\epsilon^{-1/2}$ given in Eq. (B8) with the dependence on ϵ^{-1} for a cylinder moving inside a coaxial cylinder [12].)

Because the elements of the surface of the sphere are not parallel to the walls of the cylinder, a pressure gradient will be generated in the gas between the sphere and the cylinder, and this gradient will modify the velocity gradient (B5). We have not attempted a calculation of this effect for our problem. In the absence of such a calculation it may be instructive to recall the theory of a slipper bearing. This bearing consists of a sliding block moving with constant speed v over a stationary planar guide, and inclined at a small angle to the guide [13,14]. The direction of motion is such that fluid between the plates is being dragged from the wider to the narrower opening of the bearing. When the ratio of the width of the wider opening to the width of the narrower opening is large, the velocity gradient of the fluid at the narrower opening, and at the surface of the upper plate, is approximately [13,14]

$$4v/y, \tag{B9}$$

independent of the angle of inclination. That is, an enhancement by a factor 4 of the value for parallel planes. This suggests that our estimate (B8) is a lower limit for the value of Δ.

[1] J. Pierrus and O. L. de Lange, Phys. Rev. E **56**, 2841 (1997).
[2] E. Rüchardt, Phys. Z. **30**, 58 (1929).
[3] C. G. Deacon and J. P. Whitehead, Am. J. Phys. **60**, 859 (1992).
[4] Actually, there is a phase lag between the average temperature of the gas and the displacement $x(t)$. See Eq. (29) of Ref. [1].
[5] Our Eqs. (3) and (5) follow from Eqs. (41) and (42) of Ref. [1].
[6] See, for example, J. H. Dymond and E. B. Smith, *The Virial Coefficients of Gases* (Clarendon Press, Oxford, 1969). Note that in our work the contribution of the third virial coefficient in Eq. (7) is small, and has been neglected.
[7] See, for example, E. A. Guggenheim, *Thermodynamics* (North-Holland, Amsterdam, 1950), p. 102.
[8] G. G. Stokes, Philos. Mag. **1**, 305 (1851).
[9] See, for example, A. D. Pierce, *Acoustics* (McGraw-Hill, New York, 1981), Chap. 1.
[10] *Handbuch der Physik*, edited by S. Flügge (Springer-Verlag, Berlin, 1963), Vol. 8 Pt. 2, p. 246.
[11] G. Petit Bois, *Tables of Indefinite Integrals* (Dover, New York, 1961), p. 117.
[12] See Ref. [10], p. 51.
[13] S. W. Yuan, *Foundations of Fluid Mechanics* (Prentice-Hall, Englewood Cliffs, NJ, 1967), p. 277–282.
[14] G. K. Batchelor, *An Introduction to Fluid Dynamics* (Cambridge University Press, Cambridge, 1967), pp. 219–222. Our result (B9) follows by differentiating Eq. (4.8.11) of this reference, then putting $y=d_2$ and using Eqs. (4.8.13) and (4.8.15) with $d_1 \gg d_2$.